

GT2011-46066

**OPTIMIZATION OF WIND TURBINE BLADES USING LIFTING SURFACE METHOD
AND GENETIC ALGORITHM**

Xin Shen
Shanghai Jiaotong University, 800 Dongchuan Road, Min Hang, Shanghai, 200240, China

Xiao-cheng Zhu

Zhao-hui Du

ABSTRACT

This paper describes an optimization method for the design of horizontal axis wind turbines using the lifting surface method as the performance prediction model and a genetic algorithm for optimization. The aerodynamic code for the design method is based on the lifting surface method with a prescribed wake model for the description of the wake. A micro genetic algorithm handles the decision variables of the optimization problem such as the chord and twist distribution of the blade. The scope of the optimization method is to achieve the best trade off of the following objectives: maximum of annual energy production and minimum of blade loads including thrust and blade root flap-wise moment. To illustrate how the optimization of the blade is carried out the procedure is applied to NREL Phase VI rotor. The result shows the optimization model can provide a more efficient design.

INTRODUCTION

Wind turbine rotors are unique components which not only extract power from the wind but also transfer loads to other components of the wind turbines. The aerodynamic and structure design of wind turbine rotors is a multi objective task which involves different requirements such as maximizing the rotors' annual power production and minimizing the cost of energy. The aerodynamic profiles of the blades have crucial influence on the aerodynamic efficiency of wind turbine rotors. There is an increased interest in the study of the blades with 3D meanline (swept bent blades) to improve aerodynamic efficiency and reduce the air-loads and noise of the rotors.

There have been many papers published recently for the design of wind turbine rotors. Selig et al.[1] combined a genetic algorithm with an inverse design method as an optimization method for stall-regulated horizontal-axis wind turbines. The object was to maximize the annual energy production. Fuglsang and Madsen[2] presented a numerical multi-disciplinary optimization method for design of horizontal axis wind turbines. The method included multiple constraints and the

object was the minimum cost of energy, which is determined by the design giving fatigue and extreme loads and the annual production of energy. Benini and Toffolo [3] described a multi-objective optimization method for the design of stall regulated horizontal-axis wind turbines. Their results indicated that the minimization of cost of energy (COE) required HAWTs having high AEPs (annual energy production) but low blade loads and low blade weights. Wang et al.[4] presented a design tool for optimizing wind turbine blades which is based on an aero-elastic code. The objective of the optimization model was to minimize the COE which is calculated for the AEP and the cost of the rotor. All the aerodynamic models above were based on blade element and momentum (BEM) theory. Hampsey [5] improved the optimization method by using a panel method for aerodynamic performance prediction. Burger and Hartfield [6] used the combination of the lifting surface method for aerodynamic performance prediction with a genetic algorithm for the optimization of the aerodynamic performance of HAWT blades which assumes the blades as swept blades. They implicitly remarked the importance of using a relatively higher order method for aerodynamic prediction. Lifting surface and panel methods have been widely used for the research and development of aircraft wings, aircraft propellers and ship propellers. Liu[7] developed a time domain, panel method for tidal turbine performance evaluation, design and optimization.

This paper employs a lifting surface, prescribed wake model as the aerodynamic prediction model and uses a genetic algorithm for the multi-objective optimization design of wind turbine blades. A validation is presented following the description of the lifting surface model. The optimization model is presented in the following section. To illustrate the application of the optimization model, an optimization design is obtained based on the NREL PHASE VI rotor. The new blade is a curved and swept blade with optimized chord and twist distribution.

OPTIMIZATION DESIGN PROCESS

In this paper, the design of a wind turbine blade is formulated as a multi objective optimization problem with respect to blade geometry and operation condition. For a given wind distribution, the ultimate goal of wind turbine rotor design is to obtain the maximum of energy in a year and the minimum cost of the turbine. Another important point is to choose the proper variables and constraints. In the following subsections, the design objective and variables in the optimization design model are presented. Fig. 1 illustrates the flowchart of the optimization process.

The micro-genetic algorithm is a ‘small population’ genetic algorithm that operates on the principles of natural selection to evolve the best potential solution over a number of generations to the most-fit, or optimal, solution. The 1st to report an implementation of a micro-GA was Krishnakumar[8], who used a population size of 5, a crossover rate of 1 and a mutation rate of zero. Krishnakumar[8] reported faster and better results with his micro-GA on two stationary functions and a real-world engineering control problem (a wind-shear controller task). Senecal[9] have shown that the micro genetic algorithm requires a fewer number of total function evaluations compared to classical simple genetic algorithm for their test problems. In the present work a micro genetic algorithm is chosen as the optimization algorithm.

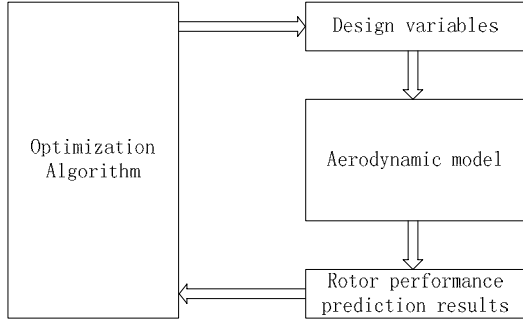


Fig. 1 Flow chart of the optimization design process

AERODYNAMIC MODEL

Aerodynamically each blade is modeled using an advanced lifting surface model which can capture the three dimensional effects on the blade. Fig. 2 presents the rotor body frame coordinates with the z-axis pointing upstream. In order to decrease the computational cost of the lifting surface model only one chord-wise panel is used and the blade is divided into finite number of span-wise panels in the present work. The bound vortices are located at 1/4 chord length and the control points are located at the 3/4 of the chord length. The trailed wake vortices comprise the near wake and far wake. The near wake extends from the bound vortices, and then rolls up into the far-wake.

The strength of each bound vortex segment circulation is determined by the boundary condition at the control point of each panel. The boundary condition implies that the incident

velocity on the blade section which is normal to the span-wise segment at the control point should be zero to prevent flow penetrate the blade:

$$\vec{V}_\infty \cdot \vec{n}_i + \vec{w}_i \cdot \vec{n}_i = 0, \quad i = 1, \dots, N_s \quad (1)$$

The velocity at the i th control point \vec{w}_i equals to the sum of the induced velocities from the bound vortices, the near wake and the far wake:

$$\vec{w} = \vec{V}_B + \vec{V}_{NW} + \vec{V}_{FW} \quad (2)$$

More detailed description of the lifting surface method can be found in Ref [10].

The shape of the far wake has substantial effect on the accuracy of the blade aerodynamic performance prediction. A prescribed wake model[11] is used for the wake geometric structure description.

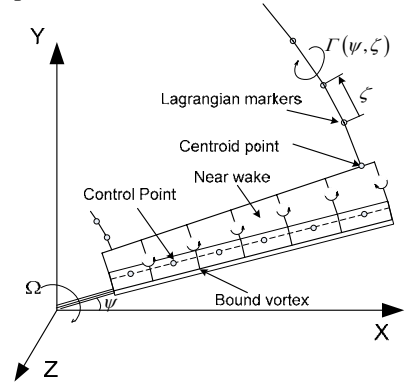


Fig. 2 Schematic of rotor coordinates and the aerodynamic blade model

VALIDATION OF THE AERODYNAMIC MODEL

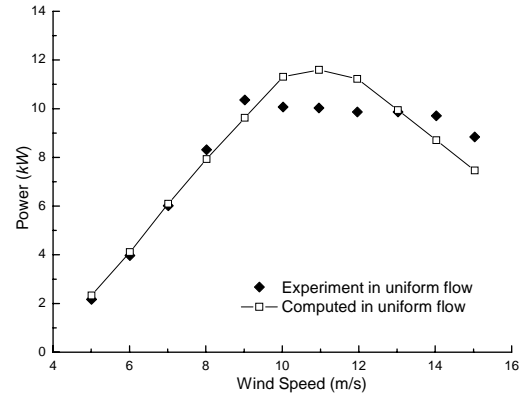


Fig. 3 comparison of predicted performance and measured data

In order to verify the numerical simulation model for the study, power output of the NREL Phase VI rotor[12] is computed without wind shear at the wind speeds from 5m/s to 15m/s. The Rotor was a two bladed stall regulated rotor tested under constant-speed (72rpm). The radius of the rotor was

5.029m and the S809 airfoil was used all along the blade. The predicted data are compared to the experimental results. As indicated in Fig. 3, the predicted aerodynamic power output is found to be in good agreement with the experimental results. The predicted power agrees well with measurements in the attached flow region (the wind speed below 9 m/s). It shows deficiency in predicted power at higher wind speed. The reason behind it is that the highly stalled flow is dominant on the blade in these cases.

To further verify the simulation, the predicted and measured C_n and C_t along the blade at the wind speed of 7m/s are shown in the Fig. 4. The data from predictions and measurements reasonably agree well.

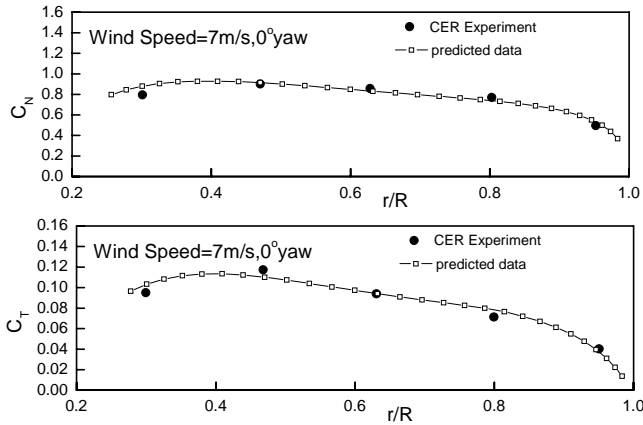


Fig. 4 Comparison of predicted and measured normal and tangential force coefficients

DESIGN OBJECTIVE

It is important and difficult to estimate the total cost of the power production. It may not only include the price of each component of the wind turbine but also the costs from operation and maintenance. A change of the load on the blade affects the turbine cost. And an improvement of the power efficiency should lower the energy cost. Instead of using the exact cost model or the sum of contributions from the main components of the wind turbine to evaluate the cost of energy, some performance characteristics (such as extreme loads, blade length and blade weight) are used for the cost evaluation. The objective function is defined as:

$$f(x) = \frac{C}{AEP} \quad (3)$$

C is the total cost and it is split into a fixed part and a variable part:

$$C = \sum_{i=1}^{NPJP} R_i (b_i + (1-b_i)P_i) \quad b_i \in [0,1] \quad (4)$$

R_i is the weight parameter for i th characteristic. And P_i is the evaluation result for i th characteristic which is determined from a reference rotor.

There are different kinds of characteristics taking into account of the cost evaluation for different types of wind turbine. Normally the magnitude of the design loads is important for the wind turbine components choosing and design. For small wind turbines, good starting performance is generally more critical than for large wind turbines. For large wind turbines, shorter diameters and lower weights are important for the rotor design. As shown in the study of ref[13], with the increasing of the diameter of wind turbines, the fatigue loads has become to the critical load cases instead of loads from extreme wind model. In the present paper, the extreme loads are not used for the cost model. 2 features (table 1) are involved in calculation of the cost. The NPJP is set to 2.

Table 1
Features involved in cost calculation

Blade root flap wise moment	M_{Flap}
Rotor thrust	N

Therefore P_i in the total cost is defined as:

$$P_1 = \frac{M_{Flap}^{opt}}{M_{Flap}^{NREL}} \quad (5)$$

where M_{Flap}^{opt} is the blade root flap wise moment of the optimum rotor and M_{Flap}^{NREL} is the blade root flap wise moment of the NREL PHASE VI rotor.

$$P_2 = \frac{N^{opt}}{N^{NREL}} \quad (6)$$

where N^{opt} is the thrust of the optimum rotor and N^{NREL} is the thrust of the NREL PHASE VI rotor.

The AEP is determined by the wind velocity of the wind site and the power curve of the wind turbine. The power curve is calculated by the lifting surface model in present paper. Throughout the NREL PHASE VI rotor design process[12], the AEP (assuming a 100% generator efficiency) was computed based on a Rayleigh wind-speed distribution having an average wind speed of 7.2 m/s (16 mph), which is representative of the windy months at NREL. In the present work, in order to compare the results of the optimum design of the rotor with the original type of the NREL PHASE VI rotor, we use the same wind velocity distribution.

DESIGN VARIABLES

Choosing the design variables is another important task for the optimization design. The key is using as few variables as possible while the chosen variables have to represent as much geometry detail and as many rotor working conditions as possible. Increasing the number of the variables will certainly increase the computation time of the optimization process. The chord, twist, rotor diameter are often use for the description of blade. Because lifting surface method can be used to predict the

aerodynamic performance of rotor with 3d geometry shape, a curved and swept blade is used in this paper.

The variables used in the paper are: chord and twist distribution, the variables for blade sweep and curve description.

Chord distribution along the blade: A Bezier curve (Fig. 5) is used for the chord length distribution along the blade. Six control points are used to define the Bezier curve. In the present work, the maximum length is at the 25% blade station, and there is a linear length transition from the hub to the maximum chord length at the 25% blade station. The six control points are placed at the 25%, 40%, 55%, 70%, 85%, 100% station. The same treatment of the root is used in the present work as the NREL PHASE VI rotor which is that the chord tapers from the maximum chord length at 25% blade span to the hub diameter of 14% blade span.

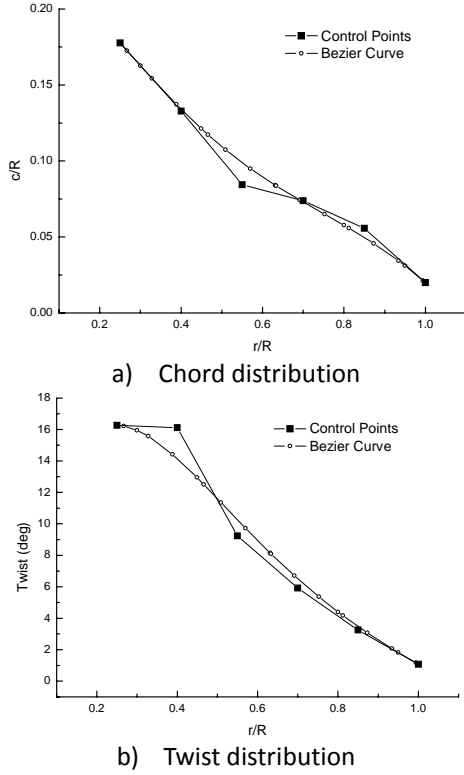


Fig. 5 Bezier curves for the chord and twist distribution description

Twist distribution along the blade: Like chord length distribution the same way is used for the twist distribution (Fig. 5).

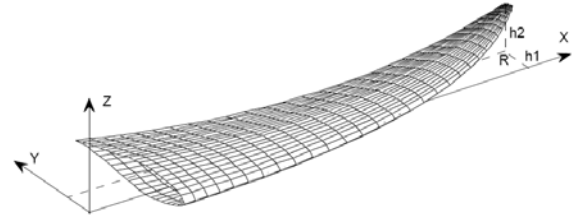


Fig. 6 Schematic of the swept-curved blade

Blade sweep and bend: The blade is defined as a backward-swept and upper curved blade. A power law function is used to describe the sweep and bend along the blade. The blade section is shifted to a new position according to the power law function given below:

$$z_{bend}(\bar{r}) = h_1 \bar{r}^{a_1} \quad (7)$$

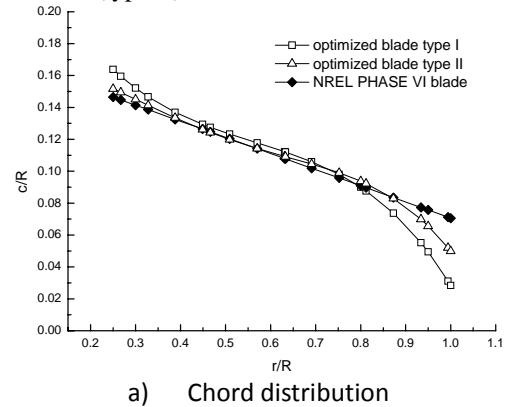
$$y_{sweep}(\bar{r}) = h_2 \bar{r}^{a_2}$$

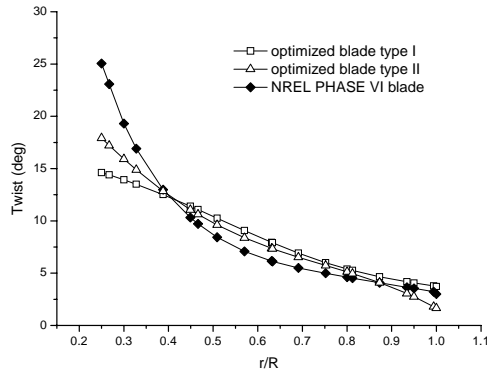
h_1 and h_2 (Fig. 6) are the maximum distance shifted which is the distance shifted at the tip of the blade. The changes of sweep and bend is governed by a_1 and a_2 where

$$\bar{r} = r / R \quad (8)$$

DESIGN RESULTS

As the case of the optimization, the same rotor is chosen in the validation section. The aim of the investigation is to find the optimum potential reduction of the blade root flap-wise moment and rotor thrust at high wind speed and the maximum of AEP. The power output and the blade root flap-wise moment are predicted by the lifting surface model. The chord and twist angle are set to be decreasing from the root to the tip of the blade. The rotor diameter, the rotation speed and the airfoil section shape are the same as the original rotor. In order to show the improvements from changes in the 3D shape of the blade, two types of optimization is employed in the present work, the 1st one (type I) is the optimized blade with swept and bent, the 2nd one (type II) without.





b) Twist distribution

Fig. 7 Chord and twist distribution of the original and optimized blades

In Fig. 7 chord and twist distributions of the original and optimized blades are shown. As it can be seen, the original blade has a linear chord distribution and the optimized blades have nonlinear chord distributions. Type I blade has larger chord length at the root and smaller at the tip. Type II blade has almost the same chord length distribution at most part of the blade until at the tip of the blade ($r/R > 80$). Both the optimized blades twist distributions are much smoother than that of the original blade. Type I blade has almost a linear twist angle distribution at most part of the blade ($r/R < 80$), and nearly the same tendency of the distribution as that of the NREL PHASE VI blade at the tip of the blade with only a little offset.

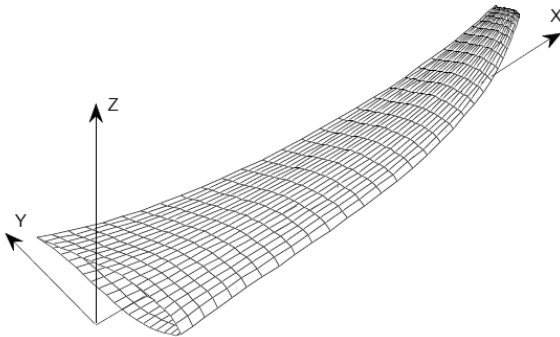


Fig. 8 Side view of the optimized swept-curved blade

Fig. 8 gives the side view of the optimized blade and the optimized shape parameters h_1 , h_2 , a_1 and a_2 are given in the following table:

Table 2
Optimized blade parameters

Blade parameter	h_1	a_1	h_2	a_2
Result(type I)	0.064	3.6475	0.0992	4.6678
Result(type II)	0	0	0	0

Fig. 9 shows the power coefficient C_p of the original and optimized rotors. Fig. 10 gives the thrust coefficient C_T of the original and optimized rotors. The power output of type I is

larger than the original blade at all wind speeds. The AEP of type I blade has been increased by about 1.65% and 0.86% for type II blade. The thrust coefficient of the optimized blade type I at all wind speeds is lower than the original blade. Under most wind speeds the type II blade has the same thrust coefficient with the original blade except when wind speeds is lower than 7m/s.

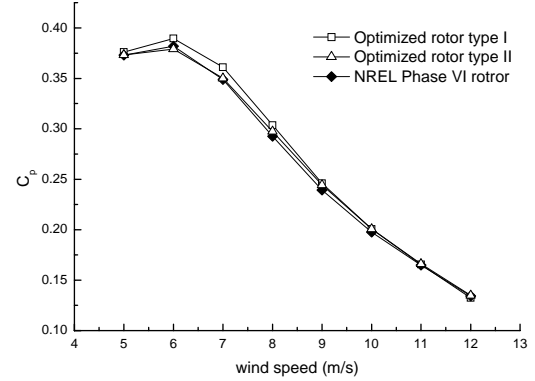


Fig. 9 Power coefficient performance of the original and optimized rotors

In order to further investigate the aerodynamic performance of the optimized blade, the effective angle of attack, the normal force, the tangential force, and the flap-wise moment distributions along the blade at wind speeds of 5m/s, 7 m/s and 9m/s are given.

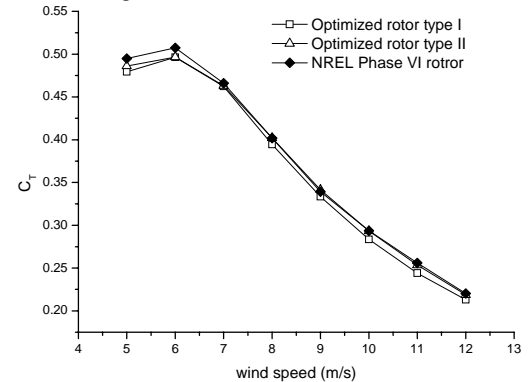


Fig. 10 Rotor thrust coefficient of the original and optimized blades

Fig. 11 gives the angle of attack distribution and Fig. 12 gives the normal and tangential forces distribution of the optimized blades and the original blade. Because of the 3D shape (sweep and bend) of the type I blade at all wind speeds it has larger angle of attack than the original blade. Type II blade has the same angle of attack with the original blade although the twist angle of type II blade at the tip is much smaller than that of the original blade due to blade tip effect. At the middle part both optimized blades have the same angle of attack. Type I blade has a bit larger angle of attack than type II blade at root.

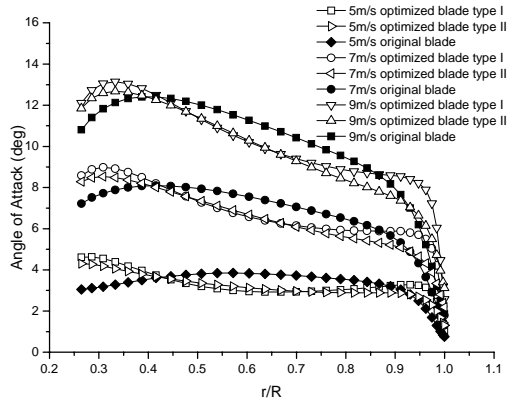


Fig. 11 Angle of attack distribution of the original and optimized blades

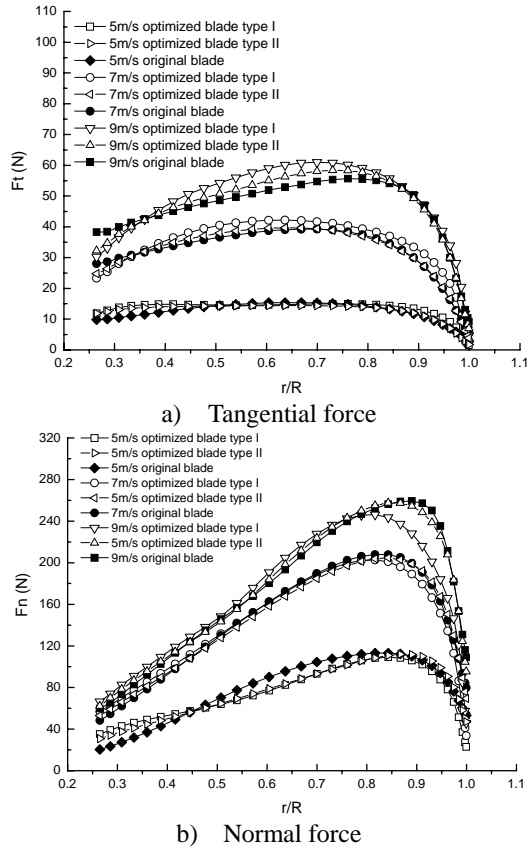


Fig. 12 Normal force and tangential force distribution of the original and optimized blades

Although the angle of attack distributions at the middle of the both optimized blades are smaller than the original blade, they have larger tangential force because of their larger twist angle. As the wind speed increases, the outboard sections of type I blade begin to produce less normal force than the optimized type II blade which is mainly caused by the 3D shape (sweep and bend) of type I blade. Both optimized blades have the same normal force at the inner sections. The blade

root flap-wise moment is one of the main causes of blade fatigue loads. Decreasing the blade root flap-wise moment may extend the mechanical life of the wind turbine.

CONCLUSION

The lifting surface model does not include any compressible and viscous effects. Therefore it shows some discrepancies in power prediction when the rotors are working at highly stalled condition. However this model proved to be valid as a whole for the aerodynamic prediction of wind turbine. It is shown that the blade with 3D shape characteristic can improve the aerodynamic performance of wind turbine rotors. The optimization object is minimum cost of energy, which is defined as the ratio between the AEP and the total cost. The total cost model depends on some main rotor performance characteristics. Both swept-curved blade and non swept-curved blade have been optimized starting from the NREL PHASE VI rotor. The results imply that the optimized swept-curved blade can get higher AEP and produce less blade root flap wise moment and rotor thrust than the optimized non-swept-curved blade.

NOMENCLATURE

a_1	Chord position function parameter
a_2	Chord position function parameter
n	Blade number
F_N	Normal force on blade
F_t	Tangential force on blade
h_1	Chord position function parameter
h_2	Chord position function parameter
M_{Flap}	Blade root flap wise moment
N	Rotor thrust
r	Position of vortex control point
\bar{r}	Relative position of vortex control point
R	Diameter of the rotor
\vec{V}_B	The induced velocity from blade
\vec{V}_{FW}	the induced velocity from far wake
\vec{V}_{NW}	The induced velocity from near wake
V_∞	free stream velocity
\bar{w}	The induced velocity on the blade
Greek Letters	

θ	Blade pitch angle
ψ	Azimuth angle
Ω	Rotor rotational speed
ψ_b	Blade azimuthal angle
ζ	Vortex age

Abbreviations

AEP	Annual energy production
NREL	U.S. National Renewable Energy Laboratory

ACKNOWLEDGMENTS

The support of the Science Foundation of Shanghai under project No. 10ZR1416000 and the Foundation of excellent academic leaders of Shanghai No.09XD1402100 are gratefully acknowledged.

REFERENCES

1. Selig, M.S. and Coverstone-Carroll, V.L., *Application of a Genetic Algorithm to Wind Turbine Design*. Journal of Energy Resources Technology, 1996. **118**(1): p. 22-28.
2. Fuglsang, P. and Madsen, H.A., *Optimization method for wind turbine rotors*. Journal of Wind Engineering and Industrial Aerodynamics, 1999. **80**(1-2): p. 191-206.
3. Benini, E. and Toffolo, A., *Optimal Design of Horizontal-Axis Wind Turbines Using Blade-Element Theory and Evolutionary Computation*. Journal of Solar Energy Engineering, 2002. **124**(4): p. 357-363.
4. Xudong, W., et al., *Shape optimization of wind turbine blades*. Wind Energy, 2009. **12**(8): p. 781-803.
5. Hampsey, M., *Multiobjective Evolutionary Optimisation of Small Wind Turbine Blades*. 2002, Ph. D. thesis, University of Newcastle
6. Burger, C. and Hartfield, R. *Wind Turbine Airfoil Performance Optimization using the Vortex Lattice Method and a Genetic Algorithm*. in AIAA 2006-4051. 2006.
7. Liu, P., *A computational hydrodynamics method for horizontal axis turbine - Panel method modeling migration from propulsion to turbine energy*. Energy, 2010. **35**(7): p. 2843-2851.
8. Krishnakumar, K. *Microgenetic algorithms for stationary and nonstationary function optimization*. in *In SPIE Proceedings: Intelligent Control and Adaptive Systems*. 1989.
9. Senecal, P., *Development of a methodology for internal combustion engine design using multi-dimensional modeling with validation through experiments*. 2000, University Microfilms International.
10. Anderson, J., *Fundamentals of aerodynamics*. Vol. 1984. 1991: McGraw-Hill New York.
11. Fisichella, C., *An improved prescribed wake analysis for wind turbine rotors*, in *Mechanical Engineering*. 2001, University of Illinois at Urbana.
12. Giguere, P. and Selig, M., *Design of a tapered and twisted blade for the NREL combined experiment rotor*. 1999. NREL/SR-500-26173
13. Malcolm, D. and Hansen, A., *WindPACT turbine rotor design study*. National Renewable Energy Laboratory, NREL/SR-500-32495, 2002.